Is a Thymine Dimer Replicated via a Transient Abasic Site Intermediate? A Comparative Study Using Non-Natural Nucleotides†

Babho Devadoss,‡ Irene Lee,‡ and Anthony J. Berdis*,§

Departments of Chemistry and Pharmacology, Case Western Reserve University, 10900 Euclid Avenue, Cleveland, Ohio 44106

Received November 27, 2006; Revised Manuscript Received January 31, 2007

ABSTRACT: UV light causes the formation of thymine dimers that can be misreplicated to induce mutagenesis and carcinogenesis. This report describes the use of a series of non-natural indolyl nucleotides in probing the ability of the high-fidelity bacteriophage T4 DNA polymerase to replicate this class of DNA lesion. Kinetic data reveal that indolyl analogues containing large π-electron surface areas are incorporated opposite the thymine dimer almost as effectively as an abasic site, a noninstructional lesion. However, there are notable differences in the kinetic parameters for each DNA lesion that indicate distinct mechanisms for their replication. For example, the rate constants for incorporation opposite a thymine dimer are considerably slower than those measured opposite an abasic site. In addition, the magnitude of these rate constants depends equally upon contributions from π-electron density and the overall size of the analogue. In contrast, binding of a nucleotide opposite a thymine dimer is directly correlated with the overall π-electron surface area of the incoming dXTP. In addition to defining the kinetics of polymerization, we also provide the first reported characterization of the enzymatic removal of natural and non-natural nucleotides paired opposite a thymine dimer through exonuclease degradation or pyrophosphorolysis activity. Surprisingly, the exonuclease activity of the bacteriophage enzyme is activated by a thymine dimer but not by an abasic site. This dichotomy suggests that the polymerase can "sense" bulky lesions to partition the damaged DNA into the exonuclease domain. The data for both nucleotide incorporation and excision are used to propose models accounting for polymerase "switching" during translesion DNA synthesis.

The ability of DNA polymerases to bypass various DNA lesions is considered to be a promutagenic event that can lead to carcinogenesis (*1*). One clear example of the causal link between the misreplication of damaged DNA and carcinogenesis is the development of skin cancer (reviewed in ref *2*). The primary causative agent of skin cancer is solar UV light that catalyzes the formation of dipyrimidine photoproducts such as cyclobutane pyrimidine dimers and pyrimidine 6-4 pyrimidone photoproducts (reviewed in ref *3*). Although these lesions are repaired by several distinct DNA repair pathways (*4*−*6*), they are also inappropriately replicated by various DNA polymerases (*7*−*9*). Indeed, insufficient repair followed by errors in replication produces characteristic mutations in dipyrimidine sequences that represent initiating events in cancer (*10*−*12*). For example, squamous cell carcinoma involves mutations in the p53 gene (*10*), while basal cell carcinoma (*11*) and melanoma (*12*) involve mutations in the PATCHED gene and the p16 gene, respectively. In each of these examples, the signature of the genetic mutation is consistent with the misreplication of UV-induced DNA lesions.

The intuitive relationship between DNA damage and cancer has spawned significant interest in the elucidation of the mechanism of nucleotide incorporation opposite and beyond a thymine dimer. Although it has been demonstrated that DNA polymerases can incorporate dNTPs opposite UV-induced DNA lesions (*7*−*9*), there are few reports providing detailed kinetic analyses of this activity. One exception, however, is the bacteriophage T7 DNA polymerase that has been extensively evaluated through kinetic and structural studies (*13*−*15*). This high-fidelity DNA polymerase is proposed to replicate a thymine dimer as a noninstructional lesion, i.e., an abasic site, as opposed to a misinstructional lesion (*13*). This conclusion was based upon comparative nucleotide selectivity studies demonstrating that the T7 DNA polymerase preferentially incorporates pyrene triphosphate (dPTP)[1] versus dATP opposite either DNA lesion (*13*, *14*). At the molecular level, this result is intriguing since the structures of these lesions differ significantly (Figure 1A). Regardless, this model was supported by structural evidence of the T7 exo$^-$ DNA polymerase bound at a thymine dimer

† This research was supported by funding from the National Institutes of Health (CA118408) and the Skin Cancer Foundation to A.J.B.

* To whom correspondence should be addressed. Telephone: (216) 368-4723. Fax: (216) 368-3395. E-mail: ajb15@cwru.edu.

‡ Department of Chemistry.

§ Department of Pharmacology.

[1] Abbreviations: dPTP, pyrene triphosphate; TBE, Tris-HCl/borate/EDTA; EDTA; ethylenediaminetetraacetate, sodium salt; dNTP, deoxynucleoside triphosphate; dXTP, non-natural deoxynucleoside triphosphate; 5-FITP, 5-fluoroindolyl-2′-deoxyriboside triphosphate; 5-AITP, 5-aminoindolyl-2′-deoxyriboside triphosphate; 5-NITP, 5-nitroindolyl-2′-deoxyriboside triphosphate; 5-NapITP, 5-naphthylindolyl-2′-deoxyriboside triphosphate; 5-AnITP, 5-anthracene indolyl-2′-deoxyriboside triphosphate; 5-PhITP, 5-phenylindolyl-2′-deoxyriboside triphosphate; 5-CE-ITP, 5-cyclohexene indolyl-2′-deoxyriboside triphosphate; 5-CH-ITP, 5-cyclohexylindolyl-2′-deoxyriboside triphosphate; gp43 exo$^-$, exonuclease-deficient mutant of the bacteriophage T4 DNA polymerase; gp43 exo$^+$, wild-type bacteriophage T4 DNA polymerase.

10.1021/bi602438t CCC: $37.00
Published on Web 03/23/2007

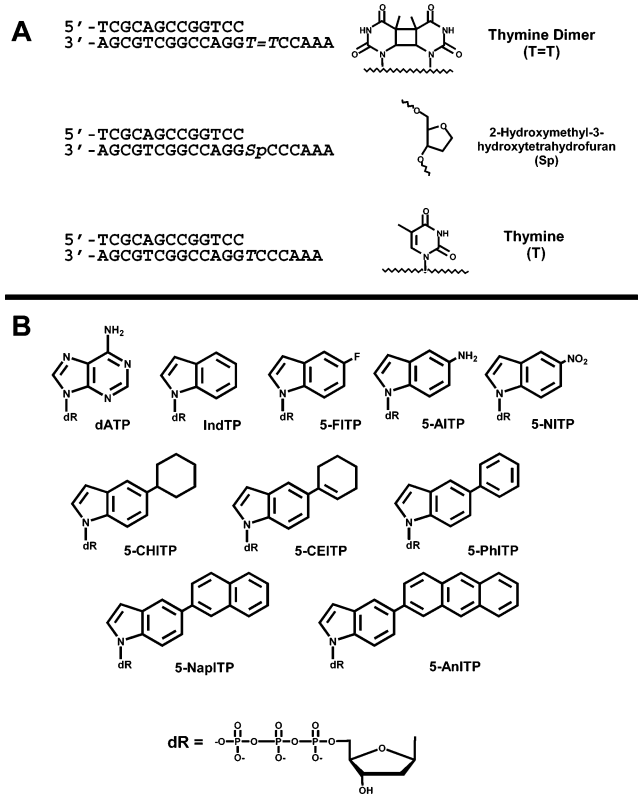

FIGURE 1: (A) Structures of 2′-deoxynucleoside triphosphates used or mentioned in this study. For convenience, dR is used to represent the deoxyribose triphosphate portion of the nucleotides. (B) Defined DNA substrates used for kinetic analysis. X in the template strand denotes a thymine dimer, a thymine, or a tetrahydrofuran moiety designed to functionally mimic an abasic site.

(*15*) in which the lesion lies outside the helical structure of DNA to create a cavity that functionally resembles an abasic site.

These observations lead us to question if similar mechanisms are employed by other high-fidelity DNA polymerases during the replication of this and other bulky DNA lesions. As such, we performed a thorough kinetic analysis comparing the ability of the bacteriophage T4 DNA polymerase (gp43) to incorporate various natural and non-natural nucleotides opposite a thymine dimer versus an abasic site. We previously demonstrated that non-natural analogues containing significant π-electron surface areas such as 5-NITP, 5-PhITP, and 5-NapITP (Figure 1B) are incorporated ~1000-fold more efficiently than analogues such as 5-AITP and 5-CHITP (Figure 1B) that have substantially smaller π-electron surface areas (*16*−*19*). These results are consistent with a model in which the overall catalytic efficiency of nucleotide incorporation is directed by the base stacking capabilities of the incoming nucleotide. In this model, the binding affinity of the incoming nucleotide is linked with its shape and hydrophobicity, while the rate constant for incorporation of these non-natural nucleotides is solely dependent on the presence of π-electron density.

These results prompted us to test the following hypothesis: if gp43 processes a thymine dimer as a transient "abasic site", then analogues such as 5-NITP, 5-PhITP, and 5-NapITP are expected to be incorporated opposite either lesion with nearly identical kinetic parameters. This report outlines the structure−activity relationships derived from monitoring the incorporation of various 5-modified indolyl nucleotides (Figure 1B) opposite a thymine dimer. These studies reveal that gp43 replicates thymine dimers and abasic sites via similar yet distinct mechanisms. This is best exemplified by the differences in the kinetic parameters measured for the incorporation of various non-natural nucleotides opposite either DNA lesion. In addition, this report evaluates the mechanisms for proofreading natural and non-natural nucleotides paired opposite either DNA lesion. Distinct differences are observed using non-natural nucleotides such as 5-PhIMP which can be excised via exonuclease and pyrophosphorolytic activity when placed opposite an abasic site but not when placed opposite a thymine dimer. The collective data set is used to develop a comprehensive model highlighting the similarities and differences in the replication of a nontemplating lesion versus a bulky miscoding DNA adduct.

MATERIALS AND METHODS

Materials. [γ-^{32}P]ATP was purchased from M. P. Bio-Medicals (Irvine, CA). Ultrapure, unlabeled dNTPs were obtained from Pharmacia. Magnesium acetate and Trizma base were obtained from Sigma. Urea, acrylamide, and bisacrylamide were from Aldrich. The oligonucleotide containing a *cis*,*syn* thymine dimer was synthesized by TriLink Biotechnologies (San Diego, CA). All other oligonucleotides, including those containing a tetrahydrofuran moiety mimicking an abasic site, were synthesized by Operon Technologies (Alameda, CA). Single-stranded and duplex DNA were purified and quantified as described previously (*20*). All other materials were obtained from commercial sources and were of the highest available quality. Wild-type gp43 and the exonuclease-deficient mutant of gp43 (Asp-219 to Ala mutation) were purified and quantified as previously described (*21*, *22*). The non-natural nucleotides used in this study were synthesized and purified as described previously (*17*−*19*).

Enzyme Assays. The assay buffer used in all kinetic studies consisted of 25 mM Tris-OAc (pH 7.5), 150 mM KOAc, and 10 mM 2-mercaptoethanol. All assays were performed at 25 °C. Polymerization reactions were monitored by analysis of the products on 20% sequencing gels (*20*). Gel images were obtained with a Packard PhosphorImager using OptiQuant supplied by the manufacturer. Product formation was quantified by measuring the ratio of ^{32}P-labeled extended to nonextended primer. The ratios of product formation are corrected for substrate in the absence of polymerase (zero point). Corrected ratios are then multiplied by the concentration of the primer−template motif used in each assay to yield total product. All concentrations are listed as final solution concentrations.

Determination of the Kinetic Rate and Dissociation Constants for Incorporation of dXTP opposite a Thymine Dimer. In most cases, a rapid quench instrument (KinTek Corp., Clarence, PA) was used to monitor the time courses for incorporation of a nucleotide opposite a thymine dimer. Experiments were performed in which 250 nM $13/20_{T=T}$-mer and variable concentrations of a nucleotide analogue (5−500 μM) were preincubated in assay buffer and mixed with 1 μM gp43 exo$^-$ and 10 mM $Mg(OAc)_2$. The reactions were quenched with 500 mM EDTA at variable times (0.005−10 s) and analyzed as described above. Data obtained

for single-turnover DNA polymerization assays were fit to eq 1.

$$y = A(1 - e^{-kt}) + C \quad (1)$$

where A is the burst amplitude, k is the observed rate constant (k_{obs}) for formation of an initial product, t is time, and C is a defined constant. Data for the dependency of k_{obs} on dXTP concentration were fit to the Michaelis−Menten equation (eq 2) to provide values corresponding to k_{pol} and K_D.

$$k_{obs} = k_{pol}[dXTP]/(K_D + [dXTP]) \quad (2)$$

where k_{obs} is the observed rate constant of the reaction, k_{pol} is the maximal polymerization rate constant, K_D is the kinetic dissociation constant for dXTP, and dXTP is the concentration of the non-natural nucleotide substrate.

Acid versus EDTA as the Quenching Agent. DNA (13/$20_{T=T}$, 250 nM) was incubated with K_D concentrations of a non-natural nucleotide and 10 mM $Mg(OAc)_2$. The reaction was then initiated with 1 μM gp43 exo$^-$ and quenched with either 500 mM EDTA or 1 M HCl at time intervals ranging from 0.1 to 10 s using a rapid quench instrument as described above. After the reaction had been quenched with 1 M HCl, 100 μL of a phenol/choloroform/isoamyl alcohol mixture was added to extract the DNA polymerase, and the pH of the aqueous phase was neutralized by addition of ~30 μL of a 1 M Tris/3 M NaOH mixture. Product formation was analyzed and quantified as described above.

Idle Turnover Measurements. DNA (13/$20_{T=T}$-mer or 13/20_{SP}-mer, 250 nM) was first preincubated with K_D concentrations of 5-PhITP (40 μM) in the presence of 30 μM dCTP. Due to the nature of the DNA substrate (Figure 1A), insertion of dCMP opposite G at position 13 in the template maintains a usable primer−template motif for the insertion of the non-natural nucleotide opposite the thymine dimer lesion (position 14). In all cases, the reaction was initiated by the addition of 1 μM gp43 exo$^+$. Reactions were quenched with 500 mM EDTA at time frames ranging from 5 to 600 s. The quenched samples were processed, and product formation was analyzed as described previously (*23*).

Exonuclease Degradation of Unmodified and Damaged DNA. Exonuclease reactions were performed under single-turnover reaction conditions in which 250 nM DNA was preincubated with 10 mM $Mg(OAc)_2$ in assay buffer, and the reaction was initiated by adding 1 μM gp43 exo$^+$. These studies include monitoring of the enzymatic hydrolysis of the following DNA substrates: 14A/$20_{T=T}$-mer, 14A/20_{SP}-mer, 13/$20_{T=T}$-mer, 13/20_{SP}-mer, and 13/20_T-mer. In all cases, a rapid quench instrument was used to quench the reactions using 500 mM EDTA at time intervals ranging from 0.003 to 2 s. Degradation products were analyzed as described above, and data points were plotted as initial substrate (13-mer) remaining as a function of time. Data for each time course were fit to eq 3 defining a first-order decay in initial substrate concentration.

$$y = Ae^{-kt} + C \quad (3)$$

where A is the amplitude of the burst phase, k is the observed rate constant for product formation, and C is the end point of the reaction.

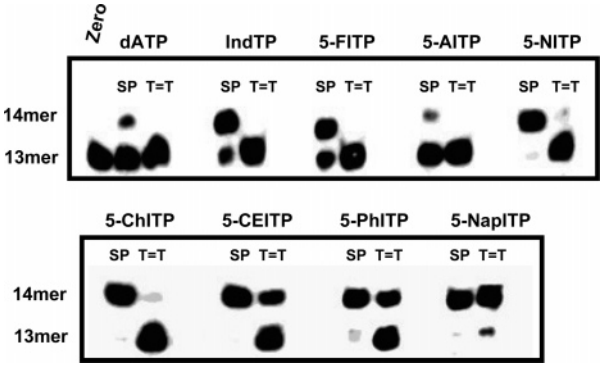

FIGURE 2: Comparing the efficiency of insertion for non-natural and natural nucleoside triphosphates opposite a thymine dimer (T=T) vs an abasic site (SP). Assays were performed as described in the text.

Pyrophosphorolysis. DNA (14A/20_T-mer, 14A/$20_{T=T}$-mer, or 14A/20_{SP}-mer, 500 nM) was first incubated with 50 nM gp43 exo$^-$ and 10 mM $Mg(OAc)_2$. The reaction was then initiated with 20 mM PP_i and quenched with 500 mM EDTA at time intervals (5−300 s). The quenched samples were processed as described above, and product formation was analyzed using protocols similar to that used to monitor the exonuclease activity of gp43 (*23*).

The pyrophosphorolytic activity of gp43 using 5-PhITP as the non-natural nucleotide was performed using a modified procedure. 13/$20_{T=T}$-mer or 13/20_{SP}-mer (500 nM) was incubated with 50 nM gp43 exo$^-$, 10 mM $Mg(OAc)_2$, and 10 μM 5-PhITP. In this case, the polymerase was allowed to enzymatically incorporate 5-PhITP opposite the DNA lesion to create the 14-mer. After ~20 min (the time required to achieve >90% conversion of 13-mer to 14-mer), pyrophosphorolysis was initiated with 20 mM PP_i. The reaction was quenched through the addition of 500 mM EDTA at time intervals (5−300 s) and the mixture processed as described above.

RESULTS AND DISCUSSION

The series of natural and non-natural nucleotides illustrated in Figure 1B were used to probe for similarities or differences in the ability of gp43 exo$^-$ to replicate a thymine dimer versus an abasic site. In either case, single-turnover conditions were used in which 1 μM gp43 exo$^-$ was added last to a preincubated solution of 50 μM dXTP and 500 nM DNA (13/$20_{T=T}$-mer or 13/20_{SP}-mer). Results comparing incorporation of a nucleotide opposite either DNA lesion are provided in Figure 2 and reveal significant differences in the efficiency of translesion DNA synthesis. For example, although IndTP, 5-FITP, and 5-AITP are readily incorporated opposite an abasic site, they are not efficiently incorporated opposite the thymine dimer. The most striking difference, however, is that dATP and 5-NITP are poorly incorporated opposite the thymine dimer. This is noteworthy since dATP and 5-NITP are efficiently incorporated opposite an abasic site (Figure 2), and this result recapitulates previously reported data (*16*, *24*). It should also be noted that of the four natural nucleotides, only dATP exhibited any incorpora-

tion opposite the thymine dimer (data not shown).[2] However, even at the highest tested concentration of dATP (1 mM), the measured rate constant of 0.007 s^{-1} is ~21-fold slower than the reported k_{pol} value of 0.15 s^{-1} measured for incorporation of dATP opposite an abasic site (*24*). In general, the difference in nucleotide utilization suggests that gp43 exo$^-$ replicates a thymine dimer via a mechanism different from that reported for an abasic site (*16*−*19*) and thus does not strictly obey the "A-rule" of translesion DNA synthesis.

There are, however, instances in which gp43 exo$^-$ utilizes certain non-natural nucleotides with comparable efficiencies regardless of DNA lesion. As illustrated in Figure 2, indolyl analogues containing large π-electron surface areas such as 5-CEITP, 5-PhITP, and 5-NapITP are incorporated opposite the thymine dimer almost as effectively as an abasic site. As such, there is an apparent dichotomy in nucleotide utilization that cannot be rationalized solely by these qualitative data. The underlying reasons for these differences in nucleotide utilization were thoroughly investigated using a quantitative kinetic approach described below.

Kinetic Parameters for Incorporation Opposite a Thymine Dimer. K_D and k_{pol} values were measured for the subset of non-natural nucleotides incorporated opposite the thymine dimer. All experiments were performed using single-turnover conditions as previously described (*16*). Representative data provided in Figure 3A show the time courses in incorporation of 5-NapITP opposite the thymine dimer. All time courses were fit to the equation for a single-exponential process to define k_{obs}, the rate constant for product formation. As shown in Figure 3B, the plot of k_{obs} versus 5-NapITP concentration is hyperbolic, and a fit of the data to the Michaelis−Menten equation yields a k_{pol} value of 6.4 ± 0.5 s^{-1} and a K_D value of 13 ± 3 μM. Identical analyses were performed with other non-natural nucleotides, and the corresponding k_{pol}, K_D, and k_{pol}/K_D values are summarized in Table 1.

Inspection of Table 1 clearly indicates that analogues such as 5-CEITP, 5 PhITP, and 5-NapITP are preferentially incorporated opposite a thymine dimer. The catalytic efficiency (k_{pol}/K_D) for these analogues is between 2 and 4 orders of magnitude greater than that for smaller analogues such as 5-AITP and 5-FITP that lack extensive π-electron density. It is striking that the overall catalytic efficiency increases as the π-electron surface area increases. In general, this variation reflects alterations in binding affinity rather than perturbations in the polymerization rate constant since the k_{pol} values for 5-CEITP, 5-PhITP, and 5-NapITP are nearly identical at ~4−6 s^{-1}. The mechanistic significance of these observations is discussed below.

The favorable incorporation of analogues containing large π-electron surface areas suggests that the thymine dimer can be processed as a noninstructional lesion since similar data were obtained for their incorporation opposite an abasic site (*17*−*19*). However, the notable variations in kinetic parameters indicate that the misreplication of each lesion occurs via a distinct mechanism. One clear example is the difference

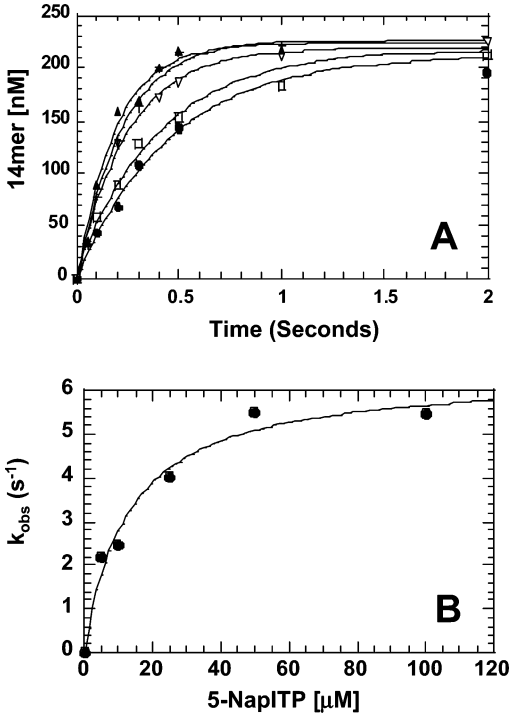

FIGURE 3: (A) Dependency of the apparent burst rate constant on the concentration 5-NapITP as measured under single-turnover conditions. Assays were performed using 1 μM gp43 exo$^-$, 250 nM 13/20 SP, 10 mM $Mg(OAc)_2$, and 5-NapITP at variable concentrations: 5 (●), 10 (□), 25 (▽), 50 (+), and 100 μM (▲). The solid lines represent the fit of the data to a single exponential. (B) The observed rate constants for incorporation (●) were plotted against 5-NapITP concentration and fit to the Michaelis−Menten equation to determine values corresponding to K_D and k_{pol}.

in binding affinities of these analogues that are dependent upon the nature of the lesion. For incorporation opposite an abasic site, the K_D values of 5-CEITP, 5-PhITP, and 5-NapITP are essentially identical at ~15 μM (*17*−*19*). During replication of a thymine dimer, however, these values vary significantly and appear to be linked with the overall π-electron surface area of the incoming dXTP. Of these three analogues, 5-NapITP has the highest binding affinity (K_D = 13 μM) which coincides with its large π-electron surface area (273 Å^2). In contrast, the smaller π-electron surface area of 5-CEITP (180.7 Å^2) arguably causes a weaker binding affinity as manifest in the 10-fold higher K_D value of 120 μM. These differences are interesting since a correlation between binding affinity and π-electron surface area is not observed during incorporation opposite an abasic site.

Differences are also detected with respect to the k_{pol} values which are again dependent upon the nature of the lesion. k_{pol} values measured with abasic site-containing DNA vary from 25 to 50 s^{-1}, while they remain essentially invariant during incorporation opposite a thymine dimer. The most dramatic effect, however, is that the rate constants for incorporation are considerably slower opposite the thymine dimer. The magnitude for this effect is largest with 5-PhITP in which the k_{pol} for an abasic site is 12-fold faster than with the thymine dimer (53 and 4.4 s^{-1}, respectively).

Perhaps the most unique kinetic behavior is again evident when we evaluate the kinetic parameters for 5-NITP.[3] The K_D of 39 μM measured opposite the thymine dimer is only 2-fold higher than the value of 18 μM measured for an abasic site (*16*). Thus, the presence of π-electron density on the

[2] Incorporation of dATP opposite a thymine dimer occurs exclusively at the 3′-end of the lesion. Sequential insertion of dATP at both the 3′- and 5′-ends of the lesion does occur, but only at dATP concentrations greater than 1 mM. However, the amount of product formed at the 5′-end of the lesion is minimal and represents <2% of complete turnover.

Table 1: Summary of Kinetic Rate and Equilibrium Constants Measured for the Insertion of dATP and 5-Substituted Indolyl-2′-deoxyriboside Triphosphates opposite a Thymine Dimer and an Abasic Site[a]

	thymine dimer			abasic site		
	K_D (μM)	k_{pol} (s^{-1})	k_{pol}/K_D (M^{-1} s^{-1})	K_D (μM)	k_{pol} (s^{-1})	k_{pol}/K_D (M^{-1} s^{-1})
dATP	ND[b]	0.007 ± 0.002[c]	<20[d]	35 ± 5	0.15 ± 0.01	4600[e]
5-NITP	39 ± 19	0.042 ± 0.006	1100	18 ± 3	126 ± 6	7000000[f]
5-FITP	ND[b]	0.030 ± 0.004[c]	<60[d]	152 ± 41	0.30 ± 0.03	2000[g]
5-CHITP	ND[b]	0.059 ± 0.004[c]	<120[d]	6.2 ± 1.3	0.46 ± 0.003	74200[h]
5-CEITP	119 ± 31	4.4 ± 0.5	36980	4.6 ± 1.0	25.1 ± 1.5	5460000[h]
5-PhITP	36 ± 13	4.4 ± 0.43	122000	14 ± 3	53 ± 4	3800000[g]
5-NapITP	13 ± 3	6.4 ± 0.5	492300	10.3 ± 4.5	27.1 ± 1.5	2631100[i]
5-AnITP	31 ± 19	1.6 ± 0.5	51600	27 ± 7	5.3 ± 0.4	200000[i]

[a] The kinetic parameters k_{pol}, K_D, and k_{pol}/K_D were obtained under single-turnover reaction conditions using 500 nM gp43 exo$^-$, 250 nM 13/$20_{T=T}$-mer, and 10 mM Mg^{2+} at varying concentrations of non-natural nucleotide triphosphate (from 5 to 500 μM). [b] Not determined. [c] k_{obs} values measured at the highest nucleotide concentration that was tested (500 μM or 1 mM). [d] Accurate values could not be determined since the lack of saturation kinetics prohibited the determination of true k_{pol} and K_D values. Thus, the reported catalytic efficiencies reflect upper estimates based upon the rate constant (k_{obs}) measured using 500 μM dXTP divided by the highest nucleotide concentration that was tested (500 μM). [e] Values taken from ref *24*. [f] Values taken from ref *16*. [g] Values taken from ref *17*. [h] Values taken from ref *19*. [i] Values taken from ref *18*.

Table 2: Summary of Kinetic Rate and Equilibrium Constants Measured for the Incorporation of dATP and 5-Substituted Indolyl-2′-deoxyriboside Triphosphates opposite a Thymine Dimer or Thymine[a]

	thymine dimer			thymine		
	K_D (μM)	k_{pol} (s^{-1})	k_{pol}/K_D (M^{-1} s^{-1})	K_D (μM)	k_{pol} (s^{-1})	k_{pol}/K_D (M^{-1} s^{-1})
dATP	ND[b]	0.007 ± 0.002[c]	<20[d]	10 ± 0.5	100 ± 10	10000000[e]
5-NITP	39 ± 19	0.042 ± 0.006	1100	9 ± 1	0.9 ± 0.1	100000[f]
5-FITP	ND[b]	0.030 ± 0.004[c]	<60[d]	141 ± 32	0.040 ± 0.003	2900[g]
5-CHITP	ND[b]	0.059 ± 0.004[c]	<120[d]	25 ± 10	0.018 ± 0.005	720[h]
5-CEITP	119 ± 31	4.4 ± 0.5	36980	63 ± 12	0.076 ± 0.005	1120[h]
5-PhITP	36 ± 13	4.4 ± 0.4	122000	25 ± 7	0.16 ± 0.01	6400[g]
5-NapITP	13 ± 3	6.4 ± 0.5	492300	16 ± 8	2.21 ± 0.4	135600[i]
5-AnITP	31 ± 19	1.6 ± 0.5	51600	29 ± 15	0.53 ± 0.11	18600[i]

[a] The kinetic parameters k_{pol}, K_D, and k_{pol}/K_D were obtained under single-turnover reaction conditions using 500 nM gp43 exo$^-$, 250 nM 13/$20_{T=T}$-mer, and 10 mM Mg^{2+} at varying concentrations of non-natural nucleotide triphosphate (from 10 to 500 μM). [b] Not determined. [c] k_{obs} values measured at the highest nucleotide concentration that was tested (500 μM or 1 mM). [d] Accurate values could not be determined since the lack of saturation kinetics prohibited the determination of true k_{pol} and K_D values. Thus, the reported catalytic efficiencies reflect upper estimates based upon the rate constant (k_{obs}) measured using 500 μM dXTP divided by the highest nucleotide concentration that was tested (500 μM). [e] Values taken from ref *20*. [f] Values taken from ref *16*. [g] Values taken from ref *17*. [h] Values taken from ref *19*. [i] Values taken from ref *18*.

incoming nucleotide appears to influence binding affinity. In contrast, the k_{pol} value of 0.042 s^{-1} measured using the thymine dimer is 3000-fold lower than the value of 126 s^{-1} measured for an abasic site (*16*). This difference suggests that the presence of π-electron density alone is insufficient to facilitate the conformational change that limits nucleotide incorporation. In fact, it appears that the k_{pol} values for incorporation opposite the thymine dimer depend equally upon contributions from both the π-electron density and the overall size of the analogue. The latter half of this finding is reminscent of the shape-complementarity model originally proposed by Kool and co-workers (reviewed in ref *25*).

[3] Initial data reported in Figure 2 indicated that 5-NITP is poorly incorporated opposite a thymine dimer. However, this low efficiency partially reflects the reaction conditions employed in this experiment, i.e., low dXTP concentration and a short reaction time of 10 s. In fact, increasing the concentration of 5-NITP and monitoring the reaction at time frames encompassing 15−600 s resulted in a dose- and time-dependent increase in the level of product formation (Supporting Information). From these experiments, a K_D of 39 ± 19 μM and a k_{pol} value of 0.042 ± 0.006 s^{-1} were measured. Similar experiments were performed using other analogues such as 5-FITP and 5-CH-ITP. In both cases, the rate and amount of primer elongation increased with the concentration of nucleotide. However, saturation kinetics were not observed even at the maximal concentration (500 μM) tested for either non-natural nucleotide. Hence, the lack of saturation prevented accurate measurements of k_{pol} and K_D values.

Of all of the non-natural nucleotides tested in this study, only 5-AnITP displays nearly identical kinetic parameters regardless of DNA lesion. For example, the K_D value of 31 μM opposite a thymine dimer is identical to that of 27 μM measured opposite an abasic site (*18*). Furthermore, the k_{pol} value of 1.6 s^{-1} for incorporation opposite a thymine dimer is only 3-fold slower than the value of 5.3 s^{-1} reported using an abasic site (*18*). While these data are consistent with the aforementioned hypothesis, it should be noted that 5-AnITP also displays unique kinetic parameters for insertion opposite templating nucleobases. Specifically, the K_D of 29 μM for incorporation opposite thymine (*18*) is identical to that of 31 μM for incorporation opposite a thymine dimer. Likewise, the k_{pol} of 0.5 s^{-1} is only 3-fold slower than the value of 1.6 s^{-1} measured for incorporation opposite a thymine dimer (*18*).

These kinetic data raised the possibility that a thymine dimer may simply be replicated as a templating nucleobase rather than as an abasic site. This was evaluated by comparing the kinetic parameters for these non-natural nucleotides opposite a thymine dimer versus an unmodified thymine (Table 2). Indeed, certain analogues lacking large π-electron surface areas (5-NITP, 5-FITP, and 5-CH-ITP) are incorporated far more efficiently opposite T than the cross-linked DNA adduct. However, other analogues such

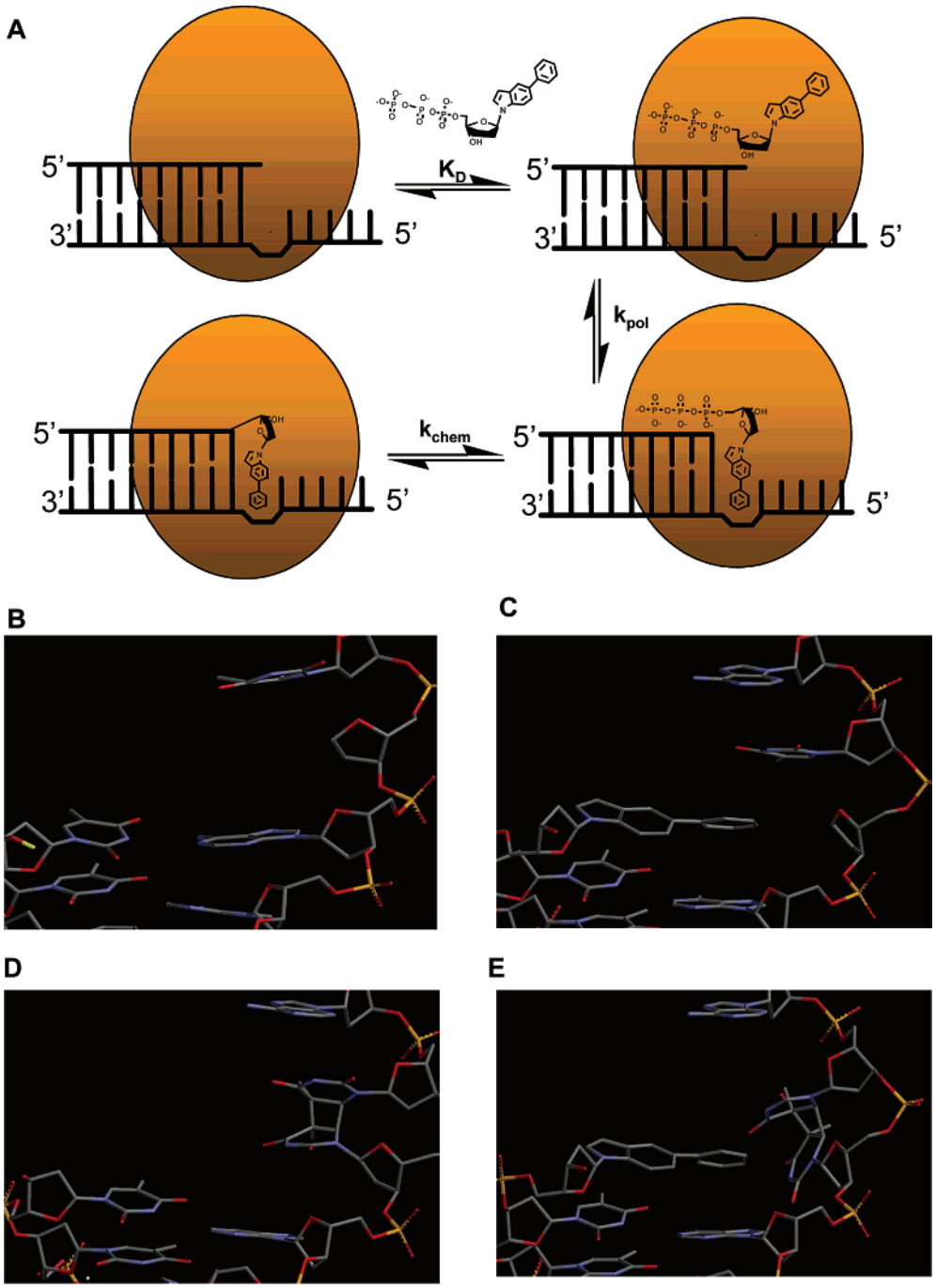

FIGURE 4: (A) Proposed model for the enzymatic incorporation of non-natural nucleotides. The first represents the binding of dNTP to the polymerase−DNA complex (K_D). After nucleotide binding, the polymerase undergoes a conformational change (k_{pol}) that is required to place the triphosphate moiety in the proximity of the positively charged amino acids as well as to stack the nucleobase portion of the incoming dNTP into the hydrophobic environment of the interior of the duplex DNA. The final stage of the catalytic cycle is phosphoryl transfer step that is required for elongation of the primer strand (k_{chem}). Panels B−E provide computer-generated models for DNA containing an abasic site (B and C) or a thymine dimer (D and E). All models were constructed using Spartan '04. (B) Computer-generated model for the structure of DNA containing an abasic site. (C) 5-Phenylindoledeoxyribose monophosphate paired opposite an abasic site in which the non-natural nucleobase is placed in an intrahelical conformation. (D) Computer-generated model for the structure of DNA containing a thymine dimer. (E) 5-Phenylindoledeoxyribose monophosphate paired opposite a thymine dimer in which the non-natural nucleobase is placed in an intrahelical conformation.

as 5-CEITP, 5-PhITP, and 5-NapITP that contain large π-electron surface areas exhibit an opposite trend as they are incorporated more effectively opposite a thymine dimer compared to thymine. In these latter instances, the increased efficiency is caused by faster k_{pol} values rather than by an enhancement in binding affinity.

These differences are significant as they suggest that gp43 does not replicate the thymine dimer strictly as an abasic site or a templating thymine. Instead, the data argue that the bulky lesion is replicated as a "hybrid" containing features common to both the nontemplating lesion and thymine. To explain such a phenomenon, we use the model illustrated in Figure 4A to propose a unified mechanism for replicating unmodified and damaged DNA. In the case of normal DNA replication, we propose that the templating nucleobase is oriented in an extrahelical position that creates a transient

"void" mimicking an abasic site (*19*). This hypothesis is based upon kinetic evidence using our non-natural nucleotides (*16*−*19*) and structural models of various DNA polymerases bound to nucleic acid (*26*−*28*). Our kinetic data indicate that large, bulky non-natural nucleotides can easily fill the void produced by this transient intermediate. In fact, the low K_D values measured for their insertion opposite a true abasic site provide further evidence of this mechanism. As seen in panels B and C of Figure 4, the non-natural nucleobase of 5-PhITP can fill the void at an abasic site and is stabilized by $\pi-\pi$ electron interactions with the penultimate base pair.

Unlike binding affinity, however, k_{pol} values are highly dependent upon the presence of a templating nucleobase. When a normal templating base is present, the k_{pol} values are slow since the shear bulk of large non-natural nucleotides hinders the facile repositioning of the templating nucleobase from an extrahelical into an intrahelical conformation. In contrast, the k_{pol} values at an abasic site are significantly faster since the lack of a templating nucleobase circumvents the need for repositioning. Furthermore, the rate of the conformational change step is dependent upon the presence of π-electron density (*19*) and is consistent with the favorable stacking interactions of the non-natural nucleobase within the void of the abasic site (Figure 4C).

The dynamics of replication of a thymine dimer are consistent with this model, especially if one considers that this lesion contains physical features common to both a templating base and a nontemplating abasic site. In this model, the 3′-T of the lesion exists predominantly, but not entirely, in an extrahelical position while the 5′-T of the lesion remains in an intrahelical position. As shown in Figure 4D, the extrahelical positioning of the 3′-T creates an intermediate resembling an abasic site. However, the covalent bond between the intrahelical 5′-T and the extrahelical 3′-T hinders the overall mobility of the lesion such that the rate constant for the prerequisite conformational change step preceding phosphoryl transfer is significantly slower compared to that for a true abasic site.

These models also indicate that the unique shape of the thymine dimer influences ground-state binding. For example, the large bulky analogue, 5-CHITP, is most likely sterically hindered from binding in a proper orientation, and this is reflected in its poor binding affinity ($K_D > 500$ μM). In contrast, analogues containing large, flat aromatic systems (5-PhITP and 5-NapITP) can interact more stably within the smaller void caused by the 3′-T (Figure 4E). Therefore, binding affinity increases as the stacking interactions between the incoming nucleotide and DNA become optimal.

We note that the aforementioned model has not been proven and that other models may exist to explain the observed differences in nucleotide utilization. A potential argument against our proposed model is the assumption that the substituent group at the C5 position of the indole ring is directed toward the opposing strand such that stacking interactions occur with the penultimate bases on both the primer and template strands. An alternative model is one in which these non-natural nucleotides exist in the *syn* conformation such that the C5 position of the indole ring is directed away from the opposing strand. Another possibility is that the indole residue simply intercalates between the penultimate and templating base as opposed to acting as a surrogate to achieve base pairing interactions. These possibilities await the results of our ongoing structural studies of various non-natural nucleotides paired opposite damaged and nondamaged DNA.

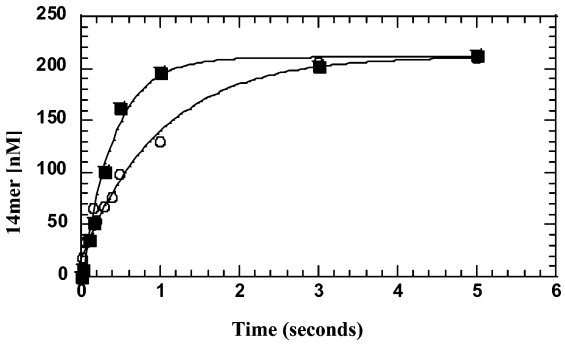

FIGURE 5: Time courses for the incorporation of 5-PhITP opposite a thymine dimer using EDTA (■) or HCl (○) as the quenching reagent. gp43 exo$^-$ (1 μM) and 5′-labeled 13/20$_{T=T}$-mer (250 nM) were preincubated, mixed with 10 mM Mg^{2+} and 30 μM 5-PhITP to initiate the reaction, and quenched with either 500 mM EDTA or 1 M HCl at variable times (0.05−5 s). After the reaction had been quenched with HCl, 100 μL of a phenol/chloroform/isoamyl alcohol mixture was added to extract the polymerase, and the pH of the aqueous phase was neutralized with the addition of a 1 M Tris/3 M NaOH mixture. Product formation was analyzed by denaturing gel electrophoresis followed by phosphorimaging analysis. An amplitude of 211 ± 6 nM and a k_{obs} of 2.51 ± 0.25 s^{-1} were obtained using EDTA as the quench, while an amplitude of 220 ± 9 nM and a k_{obs} of 0.99 ± 0.15 s^{-1} were obtained using HCl as the quenching agent.

Rate-Limiting Step for Replication of a Thymine Dimer. To further compare and contrast the mechanism of translesion DNA synthesis, a series of experiments were performed to evaluate the rate-limiting step during replication opposite a thymine dimer. Previous studies using denaturing versus nondenaturing quenching systems demonstrated that the conformational change preceding phosphoryl transfer is rate-limiting for the incorporation of non-natural nucleotides opposite an abasic site (*16*, *19*, *24*). A similar approach was used here to monitor time courses in nucleotide incorporation using EDTA (nondenaturing quench) versus HCl (denaturing agent). Any observed differences in the amount and/or rate constants in product formation using these agents can provide information regarding the existence of various enzyme forms, including E·DNA, E·DNA·dXTP, and E′·DNA·dXTP, that accumulate before the phosphoryl transfer step (E′·DNA$_{n+1}$·PP$_i$).

Initial experiments focused on the incorporation of 5-PhITP opposite the thymine dimer.[4] Time courses generated using K_D concentrations of 5-PhITP (40 μM) are provided in Figure 5 and reveal that the amplitude in product formation is independent of quenching agent (210 nM using either HCl or EDTA). The identity in burst amplitudes indicates that phosphoryl transfer is not rate-limiting for incorporation of 5-PhITP opposite the lesion. However, the difference in rate constants with EDTA and HCl (2.5 and 1 s^{-1}, respectively) indicates that incorporation opposite the thymine dimer is limited by the conformational change preceding phosphoryl transfer. A similar conclusion was made after the incorporation of 5-PhITP opposite an abasic site was monitored (*17*).

[4] Similar experiments could not be performed using dATP since this natural nucleotide is poorly incorporated opposite the thymine dimer.

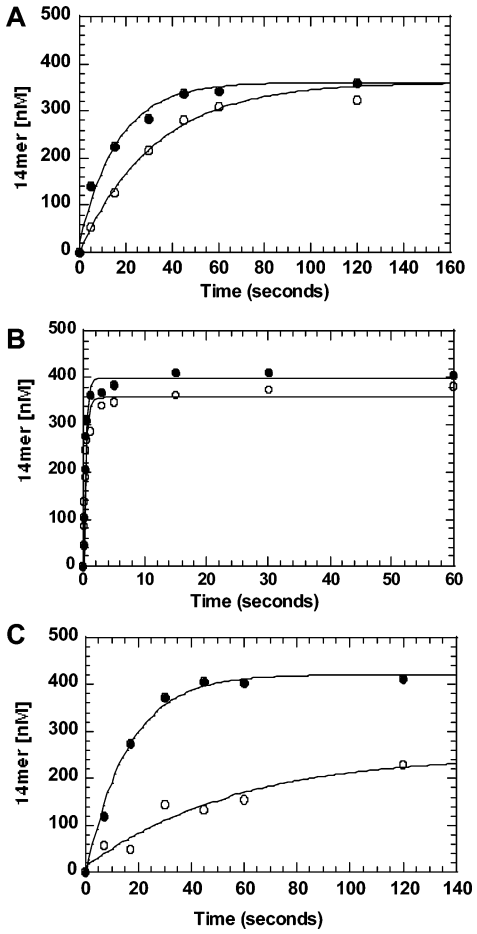

FIGURE 6: Time courses for the incorporation of 5-CH-ITP opposite a thymine dimer (A), an abasic site (B), or thymine (C) using EDTA (●) or HCl (○) as the quenching agent. Assays were performed as described in the legend of Figure 5 and the text. The following values were obtained for incorporation opposite a thymine dimer: amplitude = 360 ± 10 nM and k_{obs} = 0.060 ± 0.009 s^{-1} using EDTA, and amplitude = 360 ± 15 nM and k_{obs} = 0.031 ± 0.003 s^{-1} using HCl. The following values were obtained for incorporation opposite an abasic site: amplitude = 400 ± 10 nM and k_{obs} = 2.5 ± 0.3 s^{-1} using EDTA, and amplitude = 360 ± 20 nM and k_{obs} = 2.6 ± 0.3 s^{-1} using HCl. The following values were obtained for incorporation opposite thymine: amplitude = 420 ± 10 nM and k_{obs} = 0.063 ± 0.007 s^{-1} using EDTA, and amplitude = 250 ± 50 nM and k_{obs} = 0.018 ± 0.008 s^{-1} using HCl.

Therefore, the conformational change preceding phosphoryl transfer still remains the rate-limiting step regardless of differences in the kinetic parameters measured for incorporation of 5-PhITP opposite either lesion.

To further evaluate this mechanism, we next monitored the incorporation of 5-CHITP opposite a thymine dimer, an abasic site, and thymine using the different quenching agents. As shown in Figure 6A, the amplitude for incorporation of 5-CHITP opposite the thymine dimer is independent of quenching agent. However, the rate constant measured using EDTA is 2-fold faster than that using HCl (0.06 and 0.03 s^{-1}, respectively). The difference in rate constants again indicates that the conformational change preceding phosphoryl transfer is the rate-limiting step.

Identical experiments performed by monitoring incorporation of 5-CHITP opposite the abasic site (Figure 6B) show identical burst amplitudes and rate constants in product formation. In marked contrast, the amplitude of product formation for incorporation of 5-CHITP opposite T using HCl is reduced 40% compared to that with EDTA (Figure 6C). Furthermore, the rate constant using HCl is 3.5-fold slower than measured with EDTA (0.018 and 0.063 s^{-1}, respectively). The reduced rate constant and 40% lower amplitude indicate that the conformational change and the phosphoryl transfer step contribute equally to limiting the overall rate constant for incorporation.

These results are again interpreted with respect to the models provided in Figure 4. We propose that the conformational change step represents structural reorganization of the incoming nucleotide with the primer−template. During translesion DNA synthesis, it is easy to envision that the non-natural nucleotide can fill the void at either an abasic site or a thymine dimer and is properly oriented for phosphoryl transfer. This is not the case during incorporation opposite a templating nucleobase since both the conformational change and phosphoryl transfer steps are rate-limiting for the insertion of bulky analogues such as 5-CHITP. It is most likely that this bulky nucleobase hampers the repositioning of the primer−template which also influences the rate of the phosphoryl transfer step.

Exonuclease Proofreading Activity at a Thymine Dimer. The bacteriophage T4 polymerase possesses a vigorous exonuclease activity (*20*) that plays a significant role in maintaining fidelity (*29*). Previous work demonstrated that gp43 removes dAMP paired opposite an abasic site ~30-fold faster than when dAMP is properly paired with thymine (*23*). The faster rate constant was proposed to reflect an increase in exonuclease activity caused by distortion of the primer−template through inappropriate hydrogen bonding and stacking interactions at an abasic site. This mechanism led to the following hypothesis: if both DNA lesions are functionally identical, i.e., both are noninstructional, then the kinetics of mispair excision at a thymine dimer should be indistinguishable from that of an abasic site. This hypothesis was evaluated by comparing the kinetics by which gp43 exo^+ excises natural and non-natural nucleotides paired opposite a thymine dimer, an abasic site, or a templating thymine.

(a) Removal of Natural Nucleotides. Reactions monitoring the enzymatic hydrolysis of dAMP paired opposite the 3′-end of a thymine dimer or an abasic site were performed by employing single-turnover conditions in a rapid quench instrument as described previously (*23*). The time courses for excision of dAMP from either lesion are superimposable and best defined as a single-exponential decay (Supporting Information). Although the measured rate constants are identical, they are ~10-fold faster than the rate constant for excising dAMP paired opposite thymine (data not shown). The faster rate constants are likely caused by distortion of the primer−template junction induced by either lesion and suggest that the thymine dimer does indeed resemble an abasic site. We propose that mispairs formed at either DNA lesion enhance the enzyme's ability to partition the misaligned primer from the polymerase active site into its exonuclease domain.

To provide further evidence of DNA partitioning, we attempted to measure the idle turnover activity of the polymerase. Idle turnover is a process in which the polymerase incorporates a dNTP and then excises the inserted dNMP in the absence of the next required nucleotide triphosphate (*30*). Unfortunately, attempts to monitor the idle

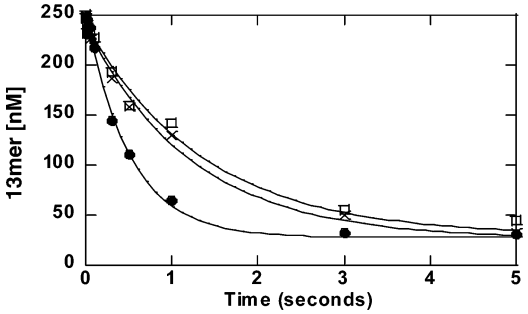

FIGURE 7: Primer degradation of DNA containing a thymine dimer (●), an abasic site (×), or thymine (□). All experiments were performed by mixing a preincubated solution of 1 μM gp43 exo$^+$ and 10 mM Mg^{2+} with 250 nM 5′-labeled DNA and 10 mM Mg^{2+} (final concentrations) and terminating the reaction at various times by the addition of 350 mM EDTA. Each time course represents an average of two independent determinations. Time courses were fit to the equation for single-exponential decay, $y = Ae^{-kt} + C$, where A is the burst amplitude, k is the observed rate constant for product formation, and C is the end point of the reaction. The rate constant for the degradation of $13/20_{T=T}$-mer is 2.0 ± 0.1 s^{-1}. The rate constants for the degradation of $13/20_T$-mer and $13/20_{SP}$-mer are 0.74 ± 0.09 and 0.82 ± 0.07 s^{-1}, respectively.

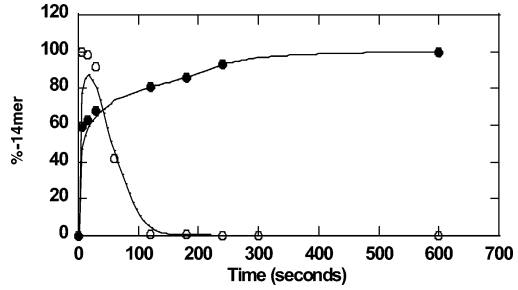

FIGURE 8: Comparison of idle turnover kinetics for insertion of 5-PhITP opposite an abasic site vs a thymine dimer. gp43 exo$^+$ (1 μM) was added last to a solution containing 250 nM 5′-labeled $13/20_{SP}$-mer (O) or $13/20_{T=T}$-mer (●), 10 mM Mg^{2+}, and 40 μM 5-PhITP. Reactions were terminated by the addition of 500 mM EDTA at time intervals ranging from 50 to 600 s. Nucleotide incorporation and excision were analyzed by denaturing gel electrophoresis.

turnover of dATP at the thymine dimer were futile since gp43 poorly incorporates this natural nucleotide opposite the lesion (vide supra). As an alternative, we directly measured the rate constant for excision of dAMP from the penultimate base pair relative to the DNA lesion using $13/20_T$-mer, $13/20_{SP}$-mer, and $13/20_{T=T}$-mer as substrates. Time courses provided in Figure 7 reveal that the exonuclease activity of gp43 is 3-fold faster with DNA containing a thymine dimer compared to DNA containing an abasic site or an unmodified thymine. The increased exonuclease activity suggests that gp43 "senses" the bulky DNA lesion and facilitates partitioning of the DNA from the polymerase site into the exonuclease active site at a higher frequency.[5]

(b) Removal of Non-Natural Nucleotides. Idle turnover experiments measured the proofreading capability of gp43 with non-natural nucleotides paired opposite the thymine dimer.[6] This activity was quantified as previously described (*23*) using a modified gel electrophoresis protocol monitoring the amount of extension (13-mer to 14-mer) and subsequent excision (14-mer to 13-mer) of the DNA as a function of time. Figure 8 provides representative time courses comparing idle turnover of 5-PhITP opposite either DNA lesion. At an abasic site, the primer is rapidly elongated to form 14-mer. This burst is followed by a short steady-state phase of product accumulation that defines the kinetics of idle turnover. During the process of nucleotide incorporation and excision, the concentration of 5-PhITP decreases until it becomes lower than the K_D value. At this point, the polymerase cannot incorporate opposite the lesion which causes degradation of the 14-mer via exonuclease activity.

Idle turnover of 5-PhITP at a thymine dimer is markedly different as the steady-state phase for 14-mer accumulation is significantly longer than that measured opposite an abasic site. The accumulation of 14-mer reflects the inability of gp43 to excise the non-natural nucleotide when it is paired opposite the thymine dimer. The difference in degradation is arguably caused by the ability of the non-natural nucleotide to stack into a dead-end complex at a thymine dimer but not at an abasic site. The models illustrated in panels C and E of Figure 4 are again useful in providing insight into the dichotomy in exonuclease activity. At an abasic site (Figure 4C), the 5-phenylindole moiety stacks very well in an intrahelical conformation and conforms satisfactorily to the overall shape and size of a natural Watson−Crick base pair (*17*). Thus, the enzyme excises the non-natural nucleotide at a rate constant comparable to that of excision of dAMP opposite T (*23*). Figure 4E also shows that 5-phenylindole can stack within the void created by the thymine dimer. However, the shape of the 5-phenylindole·thymine dimer mispair does not accurately mimic the overall shape and size of a natural base pair. At face value, one would predict that this distortion would cause the polymerase to degrade the mispair very efficiently. Indeed, we demonstrated earlier that gp43 easily excises dAMP when paired opposite a thymine dimer due to the distortion of the primer−template. However, the inability to excise 5-PhIMP argues against a model invoking simple distortion of the primer−template. We hypothesize that the proximity of the 5′-T of the lesion to the phenyl moiety of the non-natural nucleotide induces aberrant stacking interactions that can inhibit the vigorous proofreading capabilities of gp43. Further investigations are currently underway to validate this potential model.

Removal of Nucleotides via Pyrophosphorolysis. Pyrophosphorolysis, the reversal of DNA polymerization, is an important enzyme activity that can remove nucleotides from nonextendable primers in the absence of exonuclease proofreading activity (*31*). Reverse transcriptases and other viral polymerases use pyrophosphorolysis to remove various chain-terminating nucleotide analogues from their genomic material (reviewed in ref *32*). This activity is typically associated with the development of drug resistance to nucleoside analogues such as AZT and ddI (*33*−*35*). In this report, we quantified the pyrophosphorolytic activity of gp43

[5] Additional support for this mechanism comes from experiments monitoring product formation under different preincubation conditions (Supporting Information). Briefly, the rate constant in product formation is 3-fold slower when gp43 is preincubated with $13/20_{T=T}$-mer than when gp43 is preincubated with nucleotide or added last to initiate the reaction. This phenomenon is unique to the presence of the thymine dimer as identical time courses in product formation are obtained using unmodified or abasic site-containing DNA regardless of preincubation conditions (data not shown and ref *24*).

[6] Idle turnover measurements can be performed with non-natural nucleotides such as 5-PhITP as its catalytic efficiency for incorporation is high ($>10^5$ M^{-1} s^{-1}) for an abasic site or thymine dimer.

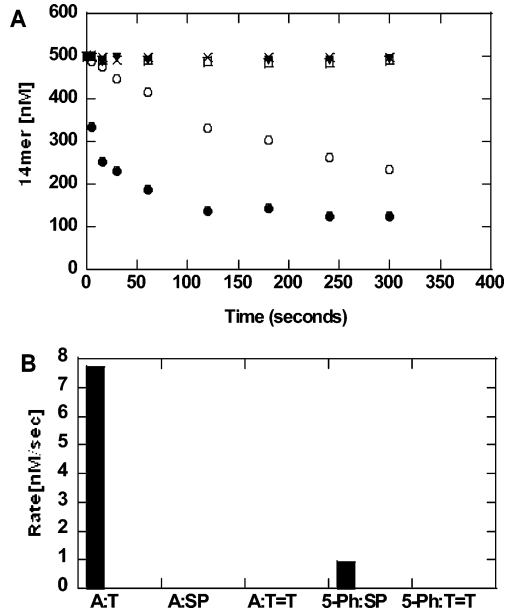

FIGURE 9: Pyrophosphorolysis activity of gp43 exo$^-$ on unmodified or damaged DNA templates. (A) Time courses for the excision of dAMP paired opposite T (●), dAMP paired opposite an abasic site (□), dAMP paired opposite a thymine dimer (×), 5-PhIMP paired opposite an abasic site (○), and 5-PhIMP paired opposite a thymine dimer (▼). Each time course represents an average of two independent determinations. (B) Comparison of the rates of pyrophosphorolysis for excision of a nucleotide opposite unmodified or damaged DNA templates. Rates were determined from the linear phase of the time courses provided in panel A.

to evaluate its potential role in excising natural and non-natural nucleotides paired opposite normal or damaged templating nucleobases. Assays monitoring the excision of dAMP were performed under pseudo-first-order reaction conditions using 500 nM DNA, 50 nM gp43 exo$^-$, and 20 mM pyrophosphate (PP_i). As shown in Figure 9A, gp43 exo$^-$ efficiently removes dAMP paired opposite T through pyrophosphorolysis and recapitulates data previously reported by Capson et al. (*20*). This datum infers that the normal primer−template motif is in a proper conformation that allows gp43 to bind it in the polymerization active site. Although the enzyme is poised for elongation, the absence of the next correct dNTP allows the enzyme to use PP_i as a substrate to reverse the polymerization reaction.

Pyrophosphorolysis activity is not observed when dATP is paired opposite either an abasic site or a thymine dimer (Figure 9A). This result is intriguing since both mispairs activate the exonuclease activity of gp43 (vide supra). The dichotomy in activity likely reflects the inability of gp43 to properly bind these mispairs in the polymerization active site. We argue that the enzyme partitions these mispairs into the exonuclease active site of gp43 and would be consistent with the enhanced exonuclease activity of gp43 when dAMP is paired opposite the 3′-T of the thymine dimer (vide supra). Partitioning of the mispair into the exonuclease active site would also explain the reluctance of the polymerase to extend beyond the mispair by incorporating opposite the 5′-T of the thymine dimer.

With this in mind, it is fascinating that 5-phenylindole can be removed by pyrophosphorolysis when placed opposite an abasic site but not when it is paired opposite a thymine dimer. These results have again been interpreted with the models provided in panels C and E of Figure 4. At an abasic site, the 5-phenylindole moiety stacks well opposite the lesion and mimics the overall shape and size of a natural Watson−Crick base pair (*17*). Thus, gp43 binds this mispair in the polymerase active site and is poised for elongation. However, in the absence of the next correct dNTP, the polymerase catalyzes pyrophosphorolysis when supplied with PP_i. Note that the rate of removal of 5-PhIMP opposite an abasic site is ∼8-fold slower than that measured for the pyrophosphorolysis of dATP paired opposite T (Figure 9B). The difference in rates could reflect the enhanced stability of the mispair through base stacking interactions of 5-PhIMP or the presence of an altered conformation that is not optimal for pyrophosphorolysis. Regardless, it is clear that the non-natural nucleotide is processed more effectively when paired opposite an abasic site compared to a thymine dimer.

Conclusions. UV radiation causes a variety of covalently modified DNA lesions, the most prevalent form of which is the *cis*,*syn* thymine dimer (reviewed in ref *3*). The hydrogen bonding groups required for base pair recognition are not altered at a thymine dimer, and this predicts that the adduct should be replicated as a miscoding lesion. However, thymine dimers also induce deformations in the helical structure of DNA (*36*) that create a cavity resembling an abasic site, a noninstructional DNA lesion. In this report, we used our series of non-natural nucleotides to demonstrate that the high-fidelity bacteriophage T4 DNA polymerase does indeed replicate the bulky lesion like an abasic site. Analogues containing large π-electron surface areas are incorporated opposite either lesion ∼1000-fold more efficiently than those analogues devoid of π-electron density. One striking example is that the catalytic efficiency for incorporation of 5-PhITP opposite a thymine dimer is ∼6000-fold higher than that for the incorporation of dATP. Similar results were obtained with the bacteriophage T7 DNA polymerase using dPTP as the non-natural nucleotide (*13*). However, the selectivity for incorporation of dPTP versus dATP opposite the thymine dimer is minimal since the reported value of ∼15 (*13*) is significantly lower that that of ∼6000 measured here using 5-PhITP and the T4 DNA polymerase. Regardless, it appears that both high-fidelity DNA polymerases use similar mechanisms to replicate a thymine dimer.

There are, however, notable differences in the kinetic parameters for these non-natural nucleotides that provide evidence that gp43 does not replicate a thymine dimer identically as an abasic site. Figure 10 provides comparative structure−activity relationships for the incorporation of several non-natural nucleotides opposite a thymine dimer versus an abasic site. During incorporation opposite an abasic site, it is clear that each of these nucleotide analogues can stack within the void present at the lesion. We argue that these stacking interactions account for the relatively equal K_D values of these analogues at an abasic site (*16*−*19*). For insertion opposite an abasic site, binding affinity is independent of π-electron density. Therefore, the lower catalytic efficiency for 5-CHITP compared to those for 5-CEITP, 5-PhITP, and 5-NITP results from a low k_{pol} value caused by the diminished π-electron surface area of 5-CHITP. As before, we argue that π-electron surface area plays the preeminent role in enhancing the rate of the conformational change step preceding phosphoryl transfer (*16*−*19*). As implied within the model provided in Figure 10, the

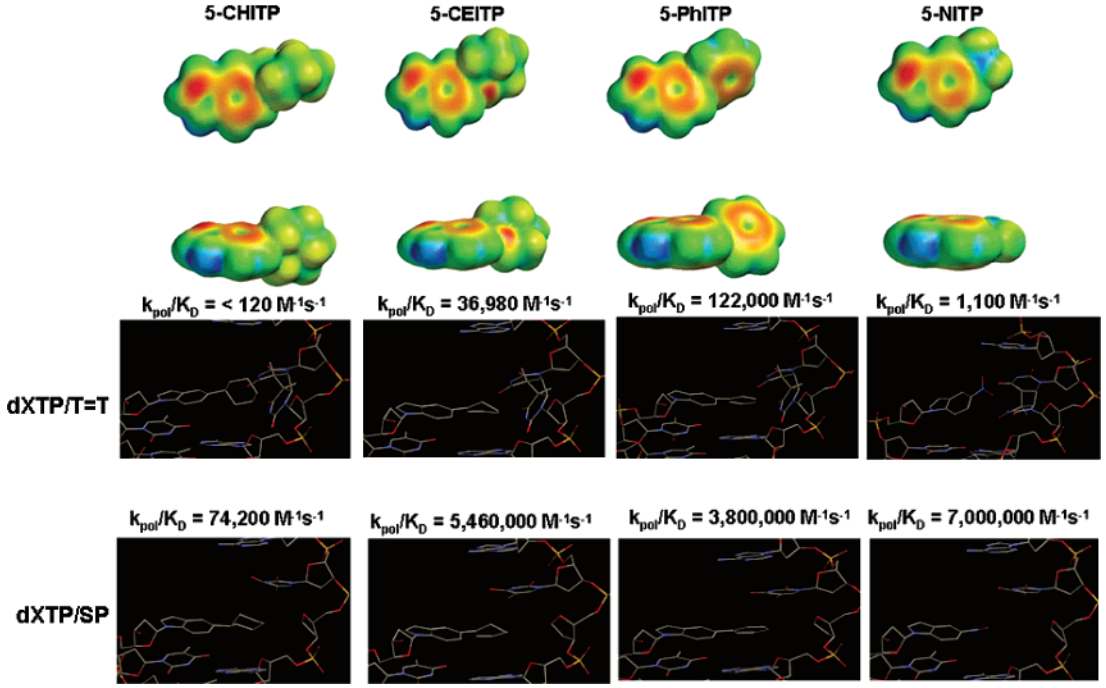

FIGURE 10: Proposed structure−activity relationships for the enzymatic incorporation of various non-natural nucleotides opposite a thymine dimer vs an abasic site. All models were constructed using Spartan '04 and are designed to illustrate the influence of π-electron surface area, shape, and size on the overall catalytic efficiency for incorporation opposite either DNA lesion. Please refer to text for further details and discussion.

π-electron surface areas of 5-CEITP, 5-PhITP, and 5-NITP are also important for stacking interactions with the penultimate base pair.

These theoretical models can also be used to explain the differences in kinetic behavior at the thymine dimer. The catalytic efficiency for incorporation opposite the thymine dimer is similar to that for an abasic site as both are linked with the overall π-electron surface area of the incoming nucleotide. However, the rate constants for the conformational change step at a thymine dimer are considerably slower compared to those for an abasic site. We interpret these differences to reflect the influence of steric hindrance imposed by the bulky lesion. In the case of 5-CHITP, it is clear that the shear bulk of the incoming nucleotide prevents optimal interactions with the bulky thymine dimer. In addition, the effect of steric hindrance diminishes as the shape of the 5-substituent group becomes more planar as the degree of π-electron density increases (compare 5-CEITP vs 5-PhITP opposite the thymine dimer). One exception is 5-NITP as it is poorly incorporated opposite the thymine dimer. Although 5-NITP is relatively planar, the model provided in Figure 10 indicates that it preferentially interacts with the 5′-end of the thymine dimer as opposed to stacking within the void caused by the thymine dimer. This difference may account for the poor incorporation of 5-NITP opposite the bulky lesion. Collectively, these analyses indicate that biophysical parameters influencing binding affinity and the rate of the conformational change step are differentially influenced by the dynamic features of the DNA lesion.

Despite differences in polymerization activity, we provide evidence that each lesion is processed similarly with respect to exonuclease proofreading and pyrophosphorolysis. The kinetics for excision of dAMP from either DNA lesion are identical and significantly faster than the excision of dAMP paired opposite an unmodified thymine. This enhancement likely reflects the enzyme's ability to partition the misaligned primer from the polymerase active site into its exonuclease domain. Similarities are also observed in the pyrophosphorolysis activity of gp43. The enzyme does not process dATP when the natural nucleotide is paired opposite either an abasic site or a thymine dimer. The lack of pyrophosphorolysis at these naturally occurring mispairs suggests that the primer−template is partitioned away from the polymerization domain. The ability to partition DNA away from the polymerization domain and into the exonuclease active site could contribute to the lack of extension beyond either class of mispair.

In this respect, both thymine dimers and abasic sites are considered to be strong replication blocks that lead to arrests in DNA synthesis (*37*−*39*). Their ability to inhibit high-fidelity DNA polymerases is proposed to reflect steric constraints imposed by the "tightness" of the active site of this family of high-fidelity DNA polymerases (*40*). The data provided here are consistent with this mechanism as geometrical constraints imposed by covalent linkage of two adjacent thymines prohibit the lesion from properly fitting within the polymerase's active site. From a biological perspective, the inability of high-fidelity polymerases to efficiently incorporate dNTPs opposite either DNA lesion is undoubtedly an important step in preventing translesion synthesis. However, we propose that the capacity of the DNA polymerase to partition mispairs away from its polymerization domain has equally important ramifications on the biological outcome of translesion DNA replication. In prokaryotes and eukaryotes, DNA replication blocks induced by diverse DNA lesions can be rescued through the action of various error-prone DNA polymerases (*41*−*46*). Relevant examples include pol η and Dpo4 which are error-prone polymerases possessing "loose" active sites (*14*, *47*) that can bypass thymine dimers (*47*, *48*). Paradoxically, the activity

of error-prone polymerases at damaged DNA ultimately allows the cell to maintain genomic fidelity. However, to perform their biological tasks, these error-prone polymerases must first gain access to the lesion by displacing the high-fidelity DNA polymerase that initially encounters it during chromosomal replication. There are several models explaining how high- and low-fidelity DNA polymerases can "switch" places with each other at a DNA lesion (*49*−*52*). Although these models differ with respect to the involvement of other proteins and/or post-translational modifications, it is clear that the high-fidelity polymerases must first stall at the DNA lesion and provide a signal to initiate these processes. We propose that signaling is achieved via the exonuclease and/or idle turnover activity of the DNA polymerase when it encounters a DNA lesion. Idle turnover, the futile cycle of nucleotide incorporation and excision, prevents the stable insertion of a dNMP opposite a template lesion and inhibits mispair elongation. Another important ramification is that the process may allow the DNA polymerase to remain "stalled" in the vicinity of the DNA lesion. In the bacteriophage T4 system, polymerase stalling may provide a direct link between replication and DNA recombination that is essential for the prevention of DNA damage (*53*). Similar mechanisms may exist in eukaryotes with respect to physically coupling the proteins involved in recombination with those at a stalled replication fork (*54*). The presence of error-prone DNA polymerases in eukaryotic systems likely provides an additional level of complexity toward the processing of damaged DNA. However, it is easy to envision that exonuclease proofreading and idle turnover may provide an essential link with these different classes of DNA polymerases. Evaluating the dynamics of this process will prove to be interesting to examine with regard to prevention of DNA damage through recombination and/or translesion DNA synthesis.

SUPPORTING INFORMATION AVAILABLE

Time courses and Michaelis−Menten plot for the incorporation of 5-NITP opposite a thymine dimer, time courses for the enzymatic hydrolysis of dAMP from DNA containing an abasic site or a thymine dimer, and time courses for incorporation of 5-PhITP opposite a thymine dimer under different preincubation conditions. This material is available free of charge via the Internet at http://pubs.acs.org.

REFERENCES

1. Loeb, L. A. (1991) Mutator phenotype may be required for multistage carcinogenesis, *Cancer Res. 51*, 3075−3079.
2. Lin, Q., Clark, A. B., McCulloch, S. D., Yuan, T., Bronson, R. T., Kunkel, T. A., and Kucherlapati, R. (2006) Increased susceptibility to UV-induced skin carcinogenesis in polymerase η-deficient mice, *Cancer Res. 66*, 87−94.
3. Pfeifer, G. P., You, Y. H., and Besaratinia, A. (2005) Mutations induced by ultraviolet light, *Mutat. Res. 571*, 19−31.
4. Garinis, G. A., Jans, J., and van der Horst, G. T. (2006) Photolyases: Capturing the light to battle skin cancer, *Future Oncol. 2*, 191−199.
5. Lloyd, R. S. (1998) Base excision repair of cyclobutane pyrimidine dimmers, *Mutat. Res. 408*, 159−170.
6. Tornaletti, S., and Pfeifer, G. P. (1996) UV damage and repair mechanisms in mammalian cells, *BioEssays 18*, 221−228.
7. Gibbs, P. E., McDonald, J., Woodgate, R., and Lawrence, C. W. (2005) The relative roles in vivo of *Saccharomyces cerevisiae* Pol η, Pol ζ, Rev1 protein and Pol32 in the bypass and mutation induction of an abasic site, T-T (6−4) photoadduct and T-T cis-syn cyclobutane dimmer, *Genetics 169*, 575−582.
8. Besaratinia, A., Synold, T. W., Xi, B., and Pfeifer, G. P. (2004) G-to-T transversions and small tandem base deletions are the hallmark of mutations induced by ultraviolet a radiation in mammalian cells, *Biochemistry 43*, 8169−8177.
9. Stary, A., Kannouche, P., Lehmann, A. R., and Sarasin, A. (2003) Role of DNA polymerase η in the UV mutation spectrum in human cells, *J. Biol. Chem. 278*, 18767−18775.
10. You, Y. H., Szabo, P. E., and Pfeifer, G. P. (2000) Cyclobutane pyrimidine dimers form preferentially at the major p53 mutational hotspot in UVB-induced mouse skin tumors, *Carcinogenesis 21*, 2113−2117.
11. Couve-Privat, S., Le Bret, M., Traiffort, E., Queille, S., Coulombe, J., Bouadjar, B., Avril, M. F., Ruat, M., Sarasin, A., and Daya-Grosjean, L. (2004) Functional analysis of novel sonic hedgehog gene mutations identified in basal cell carcinomas from xeroderma pigmentosum patients, *Cancer Res. 64*, 3559−3565.
12. Brash, D. E., Ziegler, A., Jonason, A. S., Simon, J. A., Kunala, S., and Leffell, D. J. (1996) Sunlight and sunburn in human skin cancer: p53, apoptosis, and tumor promotion, *J. Invest. Dermatol. Symp. Proc. 1*, 136−142.
13. Sun, L., Wang, M., Kool, E. T., and Taylor, J. S. (2000) Pyrene nucleotide as a mechanistic probe: Evidence for a transient abasic site-like intermediate in the bypass of dipyrimidine photoproducts by T7 DNA polymerase, *Biochemistry 39*, 14603−14610.
14. Sun, L., Zhang, K., Zhou, L., Hohler, P., Kool, E. T., Yuan, F., Wang, Z., and Taylor, J. S. (2003) Yeast pol η holds a cis-syn thymine dimer loosely in the active site during elongation opposite the 3′-T of the dimer, but tightly opposite the 5′-T, *Biochemistry 42*, 9431−9437.
15. Li, Y., Dutta, S., Doublie, S., Bdour, H. M., Taylor, J. S., and Ellenberger, T. (2004) Nucleotide insertion opposite a cis-syn thymine dimer by a replicative DNA polymerase from bacteriophage T7, *Nat. Struct. Mol. Biol. 11*, 784−790.
16. Reineks, E. Z., and Berdis, A. J. (2004) Evaluating the contribution of base stacking during translesion DNA replication, *Biochemistry 43*, 393−404.
17. Zhang, X., Lee, I., and Berdis, A. J. (2005) The use of non-natural nucleotides to probe the contributions of shape complementarity and π-electron surface area during DNA polymerization, *Biochemistry 44*, 13101−13110.
18. Zhang, X., Donnelly, A., Lee, I., and Berdis, A. J. (2006) Rational attempts to optimize non-natural nucleotides for selective incorporation opposite an abasic site, *Biochemistry 45*, 13293−13303.
19. Zhang, X., Zhou, X., Lee, I., and Berdis, A. J. (2006) Hydrophobicity, shape, and π-electron density during translesion DNA synthesis, *J. Am. Chem. Soc. 128*, 143−149.
20. Capson, T. L., Peliska, J. A., Kaboord, B. F., Frey, M. W., Lively, C., Dahlberg, M., and Benkovic, S. J. (1992) Kinetic characterization of the polymerase and exonuclease activities of the gene 43 protein of bacteriophage T4, *Biochemistry 31*, 10984−10994.
21. Frey, M. W., Nossal, N. G., Capson, T. L., and Benkovic, S. J. (1993) Construction and characterization of a bacteriophage T4 DNA polymerase deficient in 3′ → 5′ exonuclease activity, *Proc. Natl. Acad. Sci. U.S.A. 90*, 2579−2583.
22. Rush, J., and Konigsberg, W. H. (1989) Rapid purification of overexpressed T4 DNA polymerase, *Prep. Biochem. 19*, 329−340.
23. Zhang, X., Lee, I., and Berdis, A. J. (2005) A potential chemotherapeutic strategy for the selective inhibition of promutagenic DNA synthesis by nonnatural nucleotides, *Biochemistry 44*, 13111−13121.
24. Berdis, A. J. (2001) Dynamics of translesion DNA synthesis catalyzed by the bacteriophage T4 exonuclease-deficient DNA polymerase, *Biochemistry 40*, 7180−7191.
25. Kool, E. T. (2002) Active site tightness and substrate fit in DNA replication, *Annu. Rev. Biochem. 71*, 191−219.
26. Li, Y., Korolev, S., and Waksman, G. (1998) Crystal structures of open and closed forms of binary and ternary complexes of the large fragment of *Thermus aquaticus* DNA polymerase I: Structural basis for nucleotide incorporation, *EMBO J. 17*, 7514−7525.
27. Kiefer, J. R., Mao, C., Braman, J. C., and Beese, L. S. (1998) Visualizing DNA replication in a catalytically active *Bacillus* DNA polymerase crystal, *Nature 391*, 304−307.
28. Franklin, M. C., Wang, J., and Steitz, T. A. (2001) Structure of the replicating complex of a pol α family DNA polymerase, *Cell 105*, 657−667.

29. Khare, V., and Eckert, K. A. (2002) The proofreading 3′ → 5′ exonuclease activity of DNA polymerases: A kinetic barrier to translesion DNA synthesis, *Mutat. Res. 29*, 45−54.
30. Mizrahi, V., Benkovic, P. A., and Benkovic, S. J. (1986) Mechanism of the idling-turnover reaction of the large (Klenow) fragment of *Escherichia coli* DNA polymerase I, *Proc. Natl. Acad. Sci. U.S.A. 83*, 231−235.
31. Rozovskaya, T., Tarussova, N., Minassian, S., Atrazhev, A., Kukhanova, M., Krayevsky, A., Chidgeavadze, Z., and Beabealashvilli, R. (1989) Pyrophosphate analogues in pyrophosphorolysis reaction catalyzed by DNA polymerases, *FEBS Lett. 247*, 289−292.
32. Urban, S., Urban, S., Fischer, K. P., and Tyrrell, D. L. (2001) Efficient pyrophosphorolysis by a hepatitis B virus polymerase may be a primer-unblocking mechanism, *Proc. Natl. Acad. Sci. U.S.A. 98*, 4984−4989.
33. Isel, C., Ehresmann, C., Walter, P., Ehresmann, B., and Marquet, R. (2001) The emergence of different resistance mechanisms toward nucleoside inhibitors is explained by the properties of the wild type HIV-1 reverse transcriptase, *J. Biol. Chem. 276*, 48725−48732.
34. Ray, A. S., Murakami, E., Basavapathruni, A., Vaccaro, J. A., Ulrich, D., Chu, C. K., Schinazi, R. F., and Anderson, K. S. (2003) Probing the molecular mechanisms of AZT drug resistance mediated by HIV-1 reverse transcriptase using a transient kinetic analysis, *Biochemistry 42*, 8831−8841.
35. Boyer, P. L., Sarafianos, S. G., Arnold, E., and Hughes, S. H. (2002) The M184V mutation reduces the selective excision of zidovudine 5′-monophosphate (AZTMP) by the reverse transcriptase of human immunodeficiency virus type 1, *J. Virol. 76*, 3248−3256.
36. Wang, C. I., and Taylor, J. S. (1993) The trans-syn-I thymine dimer bends DNA by ≈22° and unwinds DNA by ≈15°, *Chem. Res. Toxicol. 6*, 519−523.
37. Mezzina, M., Menck, C. F., Courtin, P., and Sarasin, A. (1988) Replication of simian virus 40 DNA after UV irradiation: Evidence of growing fork blockage and single-stranded gaps in daughter strands, *J. Virol. 62*, 4249−4258.
38. Veaute, X., Mari-Giglia, G., Lawrence, C. W., and Sarasin, A. (2000) UV lesions located on the leading strand inhibit DNA replication but do not inhibit SV40 T-antigen helicase activity, *Mutat. Res. 459*, 19−28.
39. Eppink, B., Wyman, C., and Kanaar, R. (2006) Multiple interlinked mechanisms to circumvent DNA replication roadblocks, *Exp. Cell Res. 312*, 2660−2665.
40. Kim, T. W., Delaney, J. C., Essigmann, J. M., and Kool, E. T. (2005) Probing the active site tightness of DNA polymerase in subangstrom increments, *Proc. Natl. Acad. Sci. U.S.A. 102*, 15803−15808.
41. Tompkins, J. D., Nelson, J. L., Hazel, J. C., Leugers, S. L., Stumpf, J. D., and Foster, P. L. (2003) Error-prone polymerase, DNA polymerase IV, is responsible for transient hypermutation during adaptive mutation in *Escherichia coli*, *J. Bacteriol. 185*, 3469−3472.
42. Bruck, I., Goodman, M. F., and O'Donnell, M. (2003) The essential C family DnaE polymerase is error-prone and efficient at lesion bypass, *J. Biol. Chem. 278*, 44361−44638.
43. Xie, Z., Braithwaite, E., Guo, D., Zhao, B., Geacintov, N. E., and Wang, Z. (2003) Mutagenesis of benzo[a]pyrene diol epoxide in yeast: Requirement for DNA polymerase ζ and involvement of DNA polymerase η, *Biochemistry 42*, 11253−11262.
44. Bassett, E., King, N. M., Bryant, M. F., Hector, S., Pendyala, L., Chaney, S. G., and Cordeiro-Stone, M. (2004) The role of DNA polymerase η in translesion synthesis past platinum-DNA adducts in human fibroblasts, *Cancer Res. 64*, 6469−6475.
45. Kawamoto, T., Araki, K., Sonoda, E., Yamashita, Y. M., Harada, K., Kikuchi, K., Masutani, C., Hanaoka, F., Nozaki, K., Hashimoto, N., and Takeda, S. (2005) Dual roles for DNA polymerase η in homologous DNA recombination and translesion DNA synthesis, *Mol. Cell 20*, 793−799.
46. Wu, X., Takenaka, K., Sonoda, E., Hochegger, H., Kawanishi, S., Kawamoto, T., Takeda, S., and Yamazoe, M. (2006) Critical roles for polymerase ζ in cellular tolerance to nitric oxide-induced DNA damage, *Cancer Res. 66*, 748−754.
47. Mizukami, S., Kim, T. W., Helquist, S. A., and Kool, E. T. (2006) Varying DNA base-pair size in subangstrom increments: Evidence for a loose, not large, active site in low-fidelity Dpo4 polymerase, *Biochemistry 45*, 2772−2778.
48. Johnson, R. E., Washington, M. T., Prakash, S., and Prakash, L. (2000) Fidelity of human DNA polymerase η, *J. Biol. Chem. 275*, 7447−7450.
49. Indiani, C., McInerney, P., Georgescu, R., Goodman, M. F., and O'Donnell, M. (2005) A sliding-clamp toolbelt binds high- and low-fidelity DNA polymerases simultaneously, *Mol. Cell 19*, 805−815.
50. Garcia, P. B., Robledo, N. L., and Islas, A. L. (2004) Analysis of non-template-directed nucleotide addition and template switching by DNA polymerase, *Biochemistry 43*, 16515−16524.
51. McCulloch, S. D., Kokoska, R. J., and Kunkel, T. A. (2004) Efficiency, fidelity and enzymatic switching during translesion DNA synthesis, *Cell Cycle 3*, 580−583.
52. Fischhaber, P. L., and Friedberg, E. C. (2005) How are specialized (low-fidelity) eukaryotic polymerases selected and switched with high-fidelity polymerases during translesion DNA synthesis? *DNA Repair 4*, 279−283.
53. Kreuzer, K. N. (2005) Interplay between DNA replication and recombination in prokaryotes, *Annu. Rev. Microbiol. 59*, 43−67.
54. Cromie, G. A., Connelly, J. C., and Leach, D. R. (2001) Recombination at double-strand breaks and DNA ends: Conserved mechanisms from phage to humans, *Mol. Cell 8*, 1163−1174.

BI602438T